Béghein, C., Jiang, Y. and Chen, Q. 2005. "Using large eddy simulation to study particle motions in a room," *Indoor Air*, 15, 281-290.

Using Large Eddy Simulation to Study Particle Motions in a Room

Claudine Béghein[a], Yi Jiang[b], and Qingyan (Yan) Chen[c]*

[a]LEPTAB, Université de La Rochelle, Avenue Michel Crépeau, 17042 La Rochelle, France.
[b]Building Technology Program, Massachusetts Institute of Technology, 77 Massachusetts Avenue, Cambridge, MA 02139-4307, USA.
[c]School of Mechanical Engineering, Purdue University, 585 Purdue Hall, West Lafayette, IN 47907-2040, USA.
*Phone: (765) 496-7562 FAX: (765) 496-7534, Email: yanchen@purdue.edu

Abstract

As people spend most of their time in an indoor environment, it is important to predict indoor pollutant level in order to assess health risks. As particles are an important pollutant indoors, it is of great interest to study the airflow pattern and particle dispersion in buildings. This study uses large eddy simulation (LES) to predict three-dimensional and transient turbulent flows and a Lagrangian model to compute particle trajectories in a room.

The motion of three different types of solid particles in a decaying homogeneous isotropic turbulent airflow is calculated. By comparing the computed results with the experimental data from the literature, the computational method used in this investigation is found to be successful in predicting the airflow and particle trajectories in terms of the second-order statistics, such as the mean-square displacement and turbulent intensity.

This Lagrangian model is then applied to the study of particles' dispersion in a ventilated cavity with a simplified geometry for two ventilation scenarios. It is shown that light particles follow the air flow in the room and many particles are exhausted, while heavier particles deposit to the floor or/and are exhausted.

Practical implications

The results of this paper can be used to study dispersion of infectious diseases in enclosed spaces in which virus or bacteria are often attached to particles and transported to different rooms in a building through ventilation systems. In most of studies, the virus or bacteria have been considered to be gaseous phase so there is no slip between virus/bacteria and air. The results in this paper show that heavier particles are submitted to gravity and are sensitive to the ventilation strategy.

Keywords

Room airflow, particle, large eddy simulation, Lagrangian model, computational fluid dynamics

Practical implications

The results of this paper can be used to study dispersion of infectious diseases in enclosed spaces in which virus or bacteria are often attached to particles and transported to different rooms in a building through ventilation system. In most studies, the virus or bacteria have been considered

to be gaseous phase so there is no slip between virus/bacteria and air. The results in this paper show that heavier particles are submitted to gravity and are sensitive to the ventilation strategy.

Nomenclature

C_D	drag coefficient
C_{SGS}	Smagorinsky constant
d_P	particle diameter, m
f_P	response frequency of particle, s^{-1}
f_P^{-1}	characteristic time of particle, s
$F_{DRAG\ i}$	component of the drag force, in the x_i direction, N
$F_{GRAV\ i}$	component of the gravity force, in the x_i direction, N
$F_{SAF\ i}$	component of the Saffman lift force, in the x_i direction, N
g_i	component of the gravitational acceleration, in the x_i direction, m/s^2
$G(x,x')$	the filter kernel
m_P	particle mass, kg
M	mesh spacing in Snyder and Lumley's experiment (M=2.54 cm)
p	air pressure, Pa
Re_P	particle Reynolds number
u_i	component of the fluid velocity in the x_i direction, m/s
u_j	component of the fluid velocity in the x_j direction, m/s
u'	root-mean square velocity, m/s
$\bar{u}_i^*$	pseudo-velocity in the x_i direction, m/s
$\vec{u}$	air velocity, m/s
u_{max}	the maximum speed over all the grids in the physical domain, m/s
U	mean velocity along streamwise direction, m/s
$\vec{v}$	particle velocity, m/s
v_i	component of the particle velocity in the x_i direction, m/s
x_i	coordinate in i direction, m
x_j	coordinate in j direction, m
X_i	coordinate of particle, in i direction, m
Y(t)	lateral particle displacement, m
Δ_i	the filter width, m
Δ_{min}	minimum grid space, m
ν	air kinematic viscosity, m^2/s
ν_{SGS}	subgrid-scale eddy viscosity, m^2/s
ρ	air density, kg/m^3
ρ_p	particle density, kg/m^3
τ_{ij}	subgrid-scale Reynolds stresses, $(m/s)^2$

1. Introduction

In developed countries, people spend more than 90% of their time indoors. Indoor air quality is therefore an important factor of their welfare. Indoor air quality is determined by the level of indoor air contaminants, such as building materials used for internal furnishings, equipment, and

cleaning, personal activities, environmental tobacco smoke, pesticide, furnaces, soil emissions, and combustion products from cooking, as well as those from outdoors due to infiltration, such as traffic pollutants, pollen, dusts, etc. Many of the pollutants are suspended particles in air, such as dusts, smoke, fumes, and mists (ASHRAE Fundamentals, 1997). In addition, the terrorist attacks on September 11, 2001 and the following anthrax dispersion by mails have spawned concerns about various possible forms of terrorism, including airborne/aerosolized chemical and biological warfare agent attacks. The study of particle dispersion in buildings has thus received more attention at present.

To solve the indoor air quality problems and to control the particle dispersion due to a chemical/biological warfare agent attack associated with the particles, the building ventilation system plays an important role. This is because the ventilation system determines the airflow pattern in the building, and consequently, the airflow pattern decides the particle distribution and dispersion. Hence, in order to design an effective ventilation system, it is crucial to have a reliable tool that is capable to predict airflow pattern and particle distribution and dispersion in buildings.

To obtain airflow information in a building, computational fluid dynamics (CFD) modeling has become a popular method due to its informative results and low labor and equipment costs, as a result of the fast development in turbulence modeling and in computer speed and capacity. There are three commonly used CFD methods for airflow simulation: direct numerical simulation, Reynolds-averaged Navier Stokes (RANS) modeling, and large eddy simulations (LES).

Direct numerical simulation is the most accurate method. However, for airflow in a building, this method would require a high-speed and large-capacity computer that is not currently available.

When the other two CFD methods are compared, the RANS modeling seems to require less computing time than LES. However, the RANS modeling has some limitations. First, the RANS modeling has been shown to be unable to correctly predict airflow around a solid body, such as furniture and partition walls in a building. Lakehal and Rodi (1997) compared the computed results of airflow around a bluff body by using various RANS and LES models. They found that most RANS models had difficulty generating the separation region on the top surface that was observed in the experiment. Furthermore, all of the RANS models over-predicted the recirculation region behind the body. On the other hand, LES models did not encounter the problems that RANS modeling had and the LES results agreed well with the experimental data. This is probably because the large eddies generally dominate the physics of the turbulent flows. Therefore, the smallest numerical grid scale in LES is normally chosen to be 1 or 2 orders higher than the Kolmogorov microscale. Furthermore, since turbulence is inherently unsteady, the temporal accuracy of the calculation is dependent on the time step size. The time step size is determined by the stability limit of the advancement scheme and physical considerations.

Secondly, since airflow in buildings is mostly turbulent, the instantaneous velocity field will affect particle dispersion significantly (Armenio, *et al.*, 1999). Since steady RANS modeling only solves mean velocity field, a stochastic model is used to produce a fluctuating flow field (Berlemont *et al.*, 1990, Klose *et al.*, 2001, Lu *et al.*, 1993, and Pozorski and Minier, 1998) in order to take the effect of the turbulent fluctuations on the particle motions into account. Although the stochastic model can produce a fluctuation flow field, the resulting stochastic characteristics do not account for the coherence of the turbulent motions. Furthermore, the

stochastic model generally requires empirical coefficients, but the determination of those values is not a trivial issue, and it will affect the accuracy of the results.

Therefore, this investigation chooses LES to generate instantaneous flow information necessary for particle simulation. LES has been successfully applied to several airflow simulations related to buildings (Emmerich and McGrattan, 1998, Zhang and Chen, 2000, and Jiang and Chen, 2003).

The airflow computed by LES can then be used to calculate particle trajectories and dispersion patterns. There are two generic approaches for the numerical simulation of a cloud of particle trajectories and dispersion pattern in airflows: the Lagrangian and Eulerian approaches. In the Lagrangian approach, the velocity, mass and temperature histories of each particle in the cloud are calculated. The local particle motion and location represent the spatial properties of the cloud. In the Eulerian approach, the cloud of particles is considered to be a second fluid that behaves like a continuum, and equations are developed for the average properties of the particles in the cloud (Crowe, *et al.*, 1998). Each approach has its relative advantages and disadvantages depending on the nature of the flow. Compared to the Eulerian method, the main drawback of the Lagrangian approach is that a large amount of particles must be injected into the flow field in order to obtain statistically independent results. Thus, a large amount of computing time is required. The present investigation uses the Lagrangian approach to study particle dispersion patterns in buildings, because it is easier to consider the impacts of complex boundary conditions on particle motions and the approach requires no empirical coefficients such as the diffusion coefficient of particles.

This paper will detail the LES and Lagrangian particle model. It will also show the validity of the computer program by comparing the numerical results with the experimental data found from literature. This program will then be applied to the computation of particles' dispersion in an isothermal ventilated cavity.

2. Formulation

This section discusses both LES and the Lagrangian particle model.

2.1 Large Eddy Simulation

LES is based on Navier-Stokes and mass continuity equations. By filtering these equations, one would obtain the governing equations for the large-eddy motions as

$$\frac{\partial \overline{u_i}}{\partial t} + \frac{\partial}{\partial x_j}(\overline{u_i} \cdot \overline{u_j}) = -\frac{1}{\rho}\frac{\partial \overline{p}}{\partial x_i} + \nu \frac{\partial^2 \overline{u}_i}{\partial x_i \partial x_j} - \frac{\partial \tau_{ij}}{\partial x_j} \tag{1}$$

$$\frac{\partial \overline{u_i}}{\partial x_i} = 0 \tag{2}$$

The bar represents grid filtering. For example, a one-dimensional filtered velocity can be obtained from

$$\overline{u_i} = \int G(x, x')\, u_i(x)\, dx' \tag{3}$$

where $G(x,x')$, the filter kernel, is a localized function. $G(x,x')$ is large only when (x-x′) is less than a length scale or a filter width. The length scale is a length over which averaging is performed. Flow eddies larger than the length scale are "large eddies" and smaller than the length scale are "small eddies". The current study uses a box filter:

$$G(x_i)=\begin{cases}\dfrac{1}{\Delta_i} & (|x_i|\le\dfrac{\Delta_i}{2})\\ 0 & (|x_i|>\dfrac{\Delta_i}{2})\end{cases} \tag{4}$$

where Δ_i is the filter width.

The subgrid-scale Reynolds stresses in Eq. (1),

$$\tau_{ij}=\overline{u_i u_j}-\bar{u}_i\cdot\bar{u}_j \tag{5}$$

are unknown and must be modeled. The present study uses the Smagorinsky subgrid-scale model (Smagorinsky, 1963) to model the subgrid-scale Reynolds stresses. The model has been widely used since the pioneer work by Deardorff (1970). The Smagorinsky model assumes that the subgrid-scale Reynolds stresses, τ_{ij}, are proportional to the strain rate of the tensor, $\bar{S}_{ij}=\frac{1}{2}(\frac{\partial\bar{u}_i}{\partial x_j}+\frac{\partial\bar{u}_j}{\partial x_i})$, namely

$$\tau_{ij}=-2\upsilon_{SGS}\overline{S_{ij}} \tag{6}$$

where υ_{SGS} is the subgrid-scale eddy viscosity defined as

$$\upsilon_{SGS}=(C_{SGS}\Delta)^2|\bar{S}|=(C_{SGS}\Delta)^2(2\overline{S_{ij}}\cdot\overline{S_{ij}})^{\frac{1}{2}} \tag{7}$$

where C_{SGS} = 0.1 ~ 0.2 is the Smagorinsky constant, which varies according to flow type. The Smagorinsky model actually adopts the mixing length model of RANS modeling to the subgrid-scale model of LES. The Smagorinsky model has been applied to airflows around a blockage (Rodi, *et al*., 1997), mechanical ventilation in buildings (Emmerich and McGrattan, 1998), and cross natural ventilation around and in buildings (Jiang and Chen, 2002). The results agree generally with the corresponding experimental data.

2.2 Particle model

2.2.1 Lagrangian method

As discussed in the previous section, LES solves turbulent flow over the spectrum of length scales by solving the filtered form of the continuity and momentum equations for the larger scales of turbulence and by using an eddy viscosity model for the smaller scale. The flow field

determined by LES is then used to calculate particle trajectories and dispersion patterns. This study determines particle dispersion patterns with a Lagrangian method. The interaction between the carrier air and the particles has been treated as a one-way coupling, assuming that the effect of particles on the turbulent flow is negligible due to low solid loading and relatively small particle settling velocity, and that particles do not coagulate.

The Lagrangian method computes the trajectory of each particle by solving the momentum equation based on Newton's second law,

$$\frac{d(m_P v_i)}{dt} = \sum F_i \tag{8}$$

with

$$\frac{dX_i}{dt} = v_i \tag{9}$$

Momentum force is transferred between air and particles through inter-phase drag and lift forces, which can be divided into, but not limited to, the following parts: the drag force, pressure gradient force, unsteady forces which include Basset force and virtual mass force, Brownian force, and body force, such as gravity force and buoyancy force (Crowe, *et al.*, 1998). For particles with a certain size and density, some of the forces could be very small compared to others, and thus being neglected.

The current study considers only solid particles and assumes the particle shape to be sphere for simplification. The particle diameter ranges from 5 to 90 μm, and the density is at the order of 10^3 kg/m^3. As analyzed by Crowe, *et al*. (1998), when the ratio of ρ/ρ_p is of the order of 10^{-3}, the pressure gradient force can be neglected. Furthermore, according to the calculations of Hjelmfelt and Mockros (1966), the Basset force and virtual mass force become insignificant for $\rho/\rho_p \sim 10^{-3}$. Thus, these two unsteady forces can also be neglected.

If the size of a particle suspended in a fluid is very small (less than one micron), the discrete nature of molecular motion affects the motion of the particle, exhibiting a random motion due to collisions of molecules with particles. This is called Brownian motion. Since the particle sizes in this study are greater than five microns, the Brownian force is not considered. Therefore, only drag force, gravity force, buoyancy force (and Saffman lift force for the ventilated cavity) are considered in the current investigation. So the term on the right side in Eq. (8) can be expanded as

$$\sum F_i = F_{DRAG\,i} + F_{GRAV\,i}\ (+F_{SAF\,i}) \tag{10}$$

When studying particle motion in airflows, one of the most important forces is the drag force, which acts on the particle in a uniform pressure field when there is no acceleration of the relative velocity between the particle and the conveying fluid. The force is quantified by the drag coefficient, C_D, through the equation

$$F_{DRAG\,i} = -C_D \frac{\pi}{8} \rho d_P^2 \left|\vec{u} - \vec{v}\right| (v_i - u_i) \tag{11}$$

In general, the drag coefficient will depend on the particle shape and orientation with respect to the flow as well as on the flow parameters such as Reynolds number, Mach number, turbulence level, etc. Hinds (1982) computed the drag coefficient for a spherical solid particle with

$$C_D = \max\left(0.44, C_D \text{ of eq.(13)}\right) \tag{12}$$

$$C_D = \frac{24.0\left(1.0 + 0.15 Re_P^{0.687}\right)}{Re_P} \tag{13}$$

where Re_p is the particle Reynolds number :

$$Re_P = \frac{\left|\vec{u} - \vec{v}\right| d_P}{\nu} \tag{14}$$

The body forces in the current study are the gravity and the buoyancy forces, which can be expressed as

$$F_{GRAVi} = \left(\rho_P - \rho\right)\frac{\pi}{6} d_P^3 \, g_i \tag{15}$$

The shear lift force derived by Saffman (1965) is the same as in McLaughlin (1989):

$$F_{SAFi} = K\frac{\pi}{3}\sqrt{\nu}\, d_P^2\, \rho \frac{d_{ij}}{\left(d_{kl} d_{kl}\right)^{1/4}}\left(u_j - v_i\right) \tag{16}$$

$$\text{where : } K = 2.594 \text{ and } d_{ij} = \frac{1}{2}\left(\frac{\partial u_i}{\partial x_j} + \frac{\partial u_j}{\partial x_i}\right)$$

Substituting Eqs. (11), (15) and (16) into Eq. (8) and dividing by the mass of particles, m_p, on both sides, one can obtain the particle motion equation:

$$\begin{aligned} \frac{dv_i}{dt} &= -\frac{3}{4}\frac{\rho C_D}{d_p \rho_p}\left|\vec{u} - \vec{v}\right|\left(v_i - u_i\right) + \left(1 - \frac{\rho}{\rho_p}\right) g_i \quad \left(+ \frac{2K\rho\sqrt{\nu}\, d_{ij}}{\rho_P d_P \left(d_{lk} d_{kl}\right)^{1/4}}\left(u_j - v_j\right)\right) \\ &= -f_p\left(v_i - u_i\right) + \left(1 - \frac{\rho}{\rho_p}\right) g_i \quad \left(+ \frac{2K\rho\sqrt{\nu}\, d_{ij}}{\rho_P d_P \left(d_{lk} d_{kl}\right)^{1/4}}\left(u_j - v_j\right)\right) \end{aligned} \tag{17}$$

where:

$$f_p = \frac{3}{4}\frac{\rho C_D}{d_p \rho_p}\left|\vec{u} - \vec{v}\right| \tag{18}$$

is the response "frequency" of the particle to changes in flow conditions surrounding the particle.

2.2.2 Boundary conditions

The particle motion equation determines the particle trajectories in air flows. However, when particles travel through air flows in buildings, the particles may hit building walls. Therefore, the interaction between particles and building surfaces should also be considered. Several experiments have been carried out to determine whether a particle would bounce back from a wall or not (Abadie, *et al.,* 2001, Holub, *et al.,* 1988, Okuyama, *et al.*, 1986). Abadie *et al.* (2001) experimentally studied the influence of wall textures on particle deposition. They showed that particle size, wall texture and orientation are important parameters of particle deposition on walls. They noticed that 5 μm particles have a strong probability of remaining stuck on a wall texture such as a carpet which has a strong heterogeneity of surface made up of synthetic fibres with flexible nature. In addition, they highlighted that deposition increases with particle size. For the second part of our study (particles' dispersion in a ventilated cavity), we will assume the wall texture to be carpet, and thus particles will be collected by the walls (no reflection).

3. Numerical methods

This section discusses the numerical scheme employed for solving both airflow and particle equations, and determination of the time step when coupling both airflow and particle equations.

3.1 Numerical schemes

With the subgrid-scale model, the present study uses the simplified marker and cell method (SMAC) (Harlow and Welch, 1965) to solve the governing equations of LES. In order to correlate the momentum equation and the continuity equation, SMAC method first solves the momentum equations without the pressure term. So the obtained velocity, $\overline{u}_i^*$, is regarded as a pseudo-velocity.

$$\frac{\partial \overline{u}_i^*}{\partial t} + \frac{\partial}{\partial x_j}(\overline{u}_i \cdot \overline{u}_j) = \nu \frac{\partial^2 \overline{u}_i}{\partial x_j \partial x_j} - \frac{\partial \tau_{ij}}{\partial x_j} \tag{19}$$

Subtracting Eq. (1) from Eq. (19) yields:

$$\frac{\partial(\overline{u}_i^* - \overline{u}_i)}{\partial t} = \frac{1}{\rho}\frac{\partial p}{\partial x_i} \tag{20}$$

Then by placing divergence on both sides of Eq. (20) and using Eq. (2), we have

$$\frac{\partial}{\partial t}\left(\frac{\partial \overline{u}_i^*}{\partial x_i}\right) = \frac{1}{\rho}\frac{\partial^2 p}{\partial x_i^2} \tag{21}$$

Eq. (21) is a Poisson equation, which can be solved by a strong-implicit procedure (Stone, 1968). With the solution of the Poisson equation for pressure, the real velocity can be calculated with

$$\bar{u}_i = \bar{u}_i^* - \frac{\Delta t}{\rho}\frac{\partial p}{\partial x_i} \tag{22}$$

The current study uses a finite difference method to discretize the governing equations. Since the discretization of convection terms is a major source of numerical errors in LES calculation, it is very important to choose a proper scheme to discretize the convection terms. Although an upwind scheme to discretize the convection terms can provide a stable result, it introduces a built-in numerical dissipation that can be larger than the dissipation introduced by the subgrid-scale stresses. Mittal and Moin (1997) found that the upwind scheme produces poor velocity power spectra compared with the central scheme. Therefore, the current calculation uses second-order central differencing scheme to discretize the convection terms. This central differencing scheme may exhibit oscillating behavior, due to an insufficient grid resolution. Nevertheless, the convection terms should not be solved by the upwind scheme, especially the lower order of upwind scheme (Shah, 1998).

The time term in the filtered Navier Stokes equations is discretized by the explicit Adams-Bashforth scheme, which is also a second-order differencing scheme. Finally, a staggered variable configuration is used to eliminate the need for a pressure boundary condition.

The instantaneous flow velocity at the particle's location is obtained by linear interpolation of the LES instantaneous velocity field, and the particle motion equations (Eqs. (9) and (17)) are integrated with an explicit scheme: fifth order Runge-Kutta method (William, 1992).

3.2 Determination of time step size

To solve the equations of flow field and particle motion, two different time step sizes could be used: one for the flow field and the other one for the particle motion. However, in order to avoid the error due to the time interpolation, the flow field and the particle motion are advanced with the same time step, Δt. Such a time step must satisfy both the CFL condition of the flow field and the time step requirement for the particle motion. The CFL condition requires that

$$\Delta t \le \Delta t_f = \Delta_{\min} / u_{\max} \tag{23}$$

In order to simulate the correct response of the particle to the fluctuating flow field, the time step for advancement is also required to satisfy

$$\Delta t \le \Delta t_P = \varepsilon f_P^{-1} \tag{24}$$

where f_P^{-1} in Eq. (24) is the characteristic time for the particle motion, and ε is a constant and is taken to be of order $o(10^{-1})$. In practice, Δt_P can be much smaller than Δt_f for small particles. The time step size is determined by

$$\Delta t = \min(\Delta t_f, \Delta t_P) \tag{25}$$

4. Results and discussions

The above numerical method has been used to study particle dispersion in turbulent airflows. The method is first validated by an experiment measurement conducted by Snyder and Lumley (1971), who measured the dispersions of different types of particles in a channel flow. Then the validated numerical method is used to study particles' dispersion in an isothermal ventilated cavity, for two ventilation regimes.

4.1 Particle dispersion in a channel flow

The motions of small spherical solid particles are simulated numerically in a decaying homogeneous isotropic turbulent gas flow field generated by LES. Snyder and Lumley (1971) studied the particle motion in a vertical wind tunnel with air flowing upward and the gravity opposite to the flow direction, as shown in Fig. 1. The test section was 16 in. x 16 in x 16 ft (0.4 m x 0.4 m x 4.8 m). A biplane grid was made from 3/16-inch (0.476 cm) square brass rods spaced on 1-inch (2.54 cm) centers. The wind tunnel was operated with a mean speed of U = 6.55 m/sec.

In the experiment, particles were injected at the wind tunnel centerline with a mean velocity the same as the air speed, and the injection position was 20 mesh lengths (1 mesh length = 1 inch = 2.54 cm) from the biplane grid. A photographic system was used to measure the instantaneous positions of the particles at 10 separate locations. The injections were independent and about 700 measurements were made at each location. Since the flow was isotropic in planes perpendicular to the mean flow in Eulerian variables, it was isotropic in particle variables. Therefore, particle position distributions in cross sections perpendicular to the streamwise direction were circular. Since perpendicular displacements were uncorrelated with each other and had equal variances, all information was obtained from the measurements of a single component. Therefore, only the lateral particle displacements, Y(t), were measured. In addition, the turbulent intensity of the airflow in the tunnel was also measured.

In the numerical simulation, a biplane grid, which had the same geometry as that in the experiment, was placed in the windward direction to generate the isotropic and homogeneous airflow field. The smallest grid size was same as the size of the brass rods, 3/16-inch (0.476 cm). A non-uniform grid system was used, and the grid numbers were 200 × 67 × 67 along streamwise direction, x, and lateral directions, y and z. The time step size was 0.0002 seconds, determined by Eq. (25). Fig. 2 shows the decay of root-mean-square velocity fluctuation. Please note that in LES, the root-mean-square velocity of the flow is calculated as:

$$u' = \sqrt{\frac{\sum_{k=1}^{N} (u_k - u_{ave})^2}{N}} \qquad (26)$$

where u_k is the instantaneous flow velocity at the k-th time step, and u_{ave} is the average flow velocity over N time steps. The LES results agree well with the experimental data, which means LES can correctly simulate the airflow field.

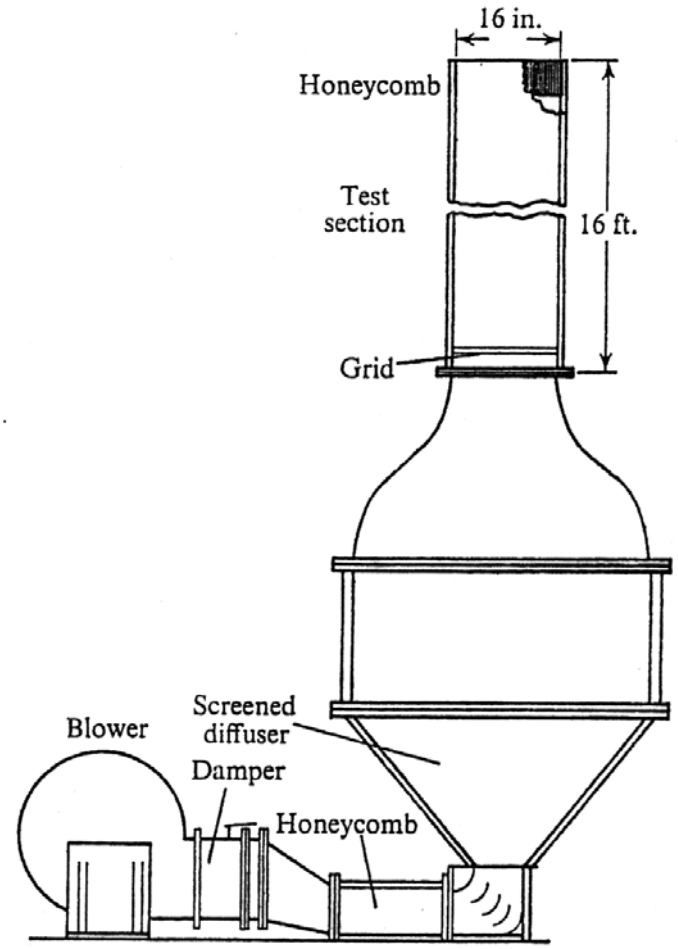

Fig. 1 The wind tunnel (Snyder and Lumley 1971)

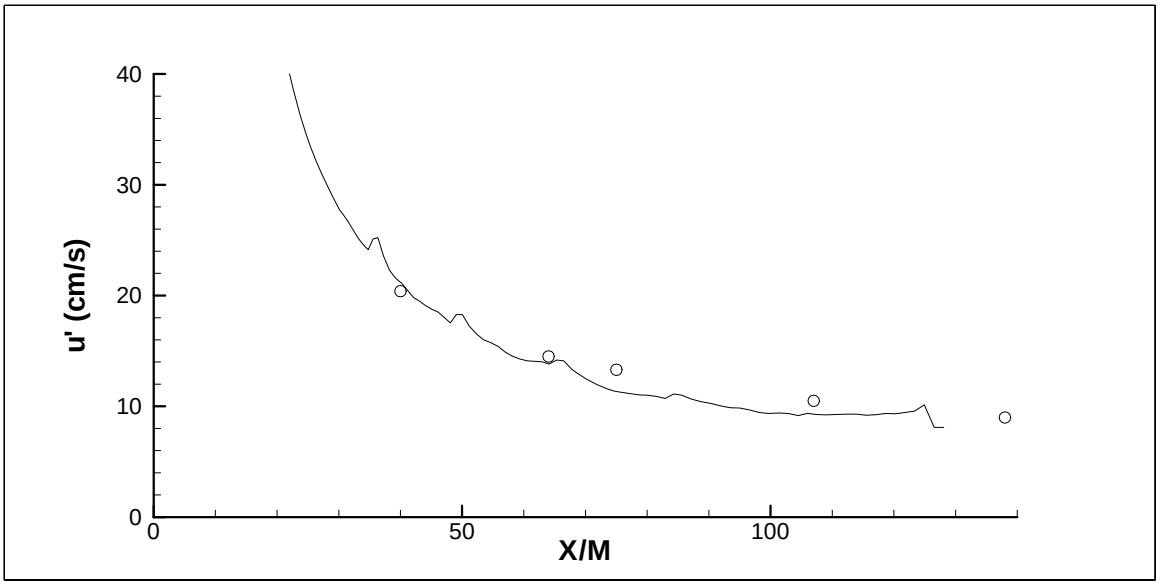

Fig. 2 Decay of the root-mean-square velocity fluctuation along the streamwise direction (M : 1 mesh length = 2.54 cm). Solid line: LES result; circle: Experimental data.

This numerical investigation studied three different types of particles: hollow glass particles with a diameter of 46.5 μm and density of 260 kg/m^3, corn particles with a diameter of 87 μm and density of 1000 kg/m^3, and copper particles with a diameter of 46.5 μm and density of 8900 kg/m^3. For each type of particles, one thousand samples were introduced to the centerline of the flow field independently 20 mesh lengths from the biplane grid with a mean velocity the same as the tunnel speed. The streamwise direction is the x-direction. Particles are submitted to the drag force (Eq. (11)), and to the gravity force (Eq. (15)) opposite to the streamwise direction. In this experiment (and thus in this simulation), there is no deposition of particles. The magnitude of the velocity difference between the local fluid point and the particle, $\left|\vec{u}-\vec{v}\right|$, increases to a maximum value and then decays with time. Since the time required for $\left|\vec{u}-\vec{v}\right|$ to reach the maximum is of the same order as the particle's characteristic time, f_P^{-1} (in Eq. (18)), particles with larger density and size would require longer time to reach the maximum than those with smaller density and size. Riley and Patterson (1974) pointed out that once $\left|\vec{u}-\vec{v}\right|$ reaches the maximum value, the statistical properties of the particle motion are free from the effect of initial condition and can be computed. In the experiment, the position for a given particle obtained by the first camera, which was located at (X/M) = 68.4 (where M is the mesh length, M = 2.54 cm), was chosen to be the reference position for that particle. In the simulation, the reference positions for the computation of the statistical properties of the particle motion were set at (X/M) = 30 – 64 , depending on different values of f_P^{-1}.

Fig. 3 shows the temporal evolution of the mean-square displacements of three different types of particles from present study and those obtained from the experiments. Again, the computational results are in good agreement with the experimental data. This Lagrangian model can thus be used with confidence for investigating particles' dispersion in a ventilated cavity.

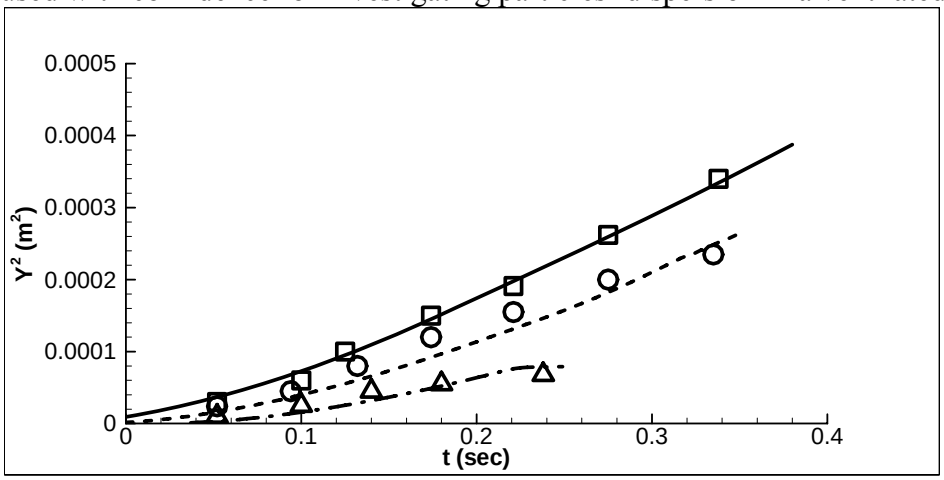

Fig. 3 Comparison of the development of the mean-square displacement of the particles between the LES results (lines) and the experimental results (symbols). Solid line: LES results for hollow particles; dashed line: LES results for corn particles; dash-dot line: LES results for copper particles; squares: experimental results for hollow particles; circles: experimental results for corn particles; deltas: experimental results for copper particles.

4.2 Particle dispersion in a ventilated room

The application case considered in this paragraph is a qualitative analysis of particles' dispersion in an isothermal ventilated room. Since the computation of particles' trajectories requires a dense grid and small time steps, the geometry of the room is simplified : the inlet and outlet are located along the left and right vertical walls (see Fig. 4). Two ventilation regimes are taken into consideration:

- One with the inlet in the lower part of the left wall (0.31 m. above the floor) and the outlet in the upper part of the right wall (0.31 m. beneath the ceiling), denoted Case (A) in Fig. 4
- One with the inlet in the upper part of the left wall and the outlet in the lower part of the right wall, denoted Case (B) in Fig. 4

The room dimensions are : length × width × height = 2.5m. × 2.5m. × 2.5m., the inlet and outlet heights are 0.07m., the supply air velocity is 0.886 m/s. The flow Reynolds number is 4130, based on inlet height. The Smagorinsky model was used to compute the instantaneous turbulent flow. The flow domain was discretized into a non uniform mesh of 266418 (57 (x) × 82 (y) × 57 (z)) cells. The time step used to solve the equations of flow field was 0.001 s. For these two configurations, a cloud of particles (1000 particles) was injected in the middle of the inlet at the same time, the initial velocity of particles was the same as the local air velocity. Particles' density was 1000 kg/m^3 , and two particles' diameters were selected: 5 µm and 20 µm. Particles were submitted to the drag force (Eq. (11)), to the gravity and buoyancy forces (Eq. (15)), and to the shear lift force (Eq. (16)). To solve the equations of particle motion, the time step was decreased to 0.0001 s. In addition, since the computations take a large amount of time, we assumed as explained in paragraph 2.2.2 that walls were covered with an absorbing texture (such as a carpet) and thus that particles were attached to walls when they contacted the surfaces. No rebound occurred, particles were stuck on the walls, and due to the low velocity of the flow, particles could not be resuspended into room air. Although these cases are simple ones, the computational cost was quite high. For each case studied, it took about 19 days on an IBM SP to compute particles' trajectories for a period of 38 s.

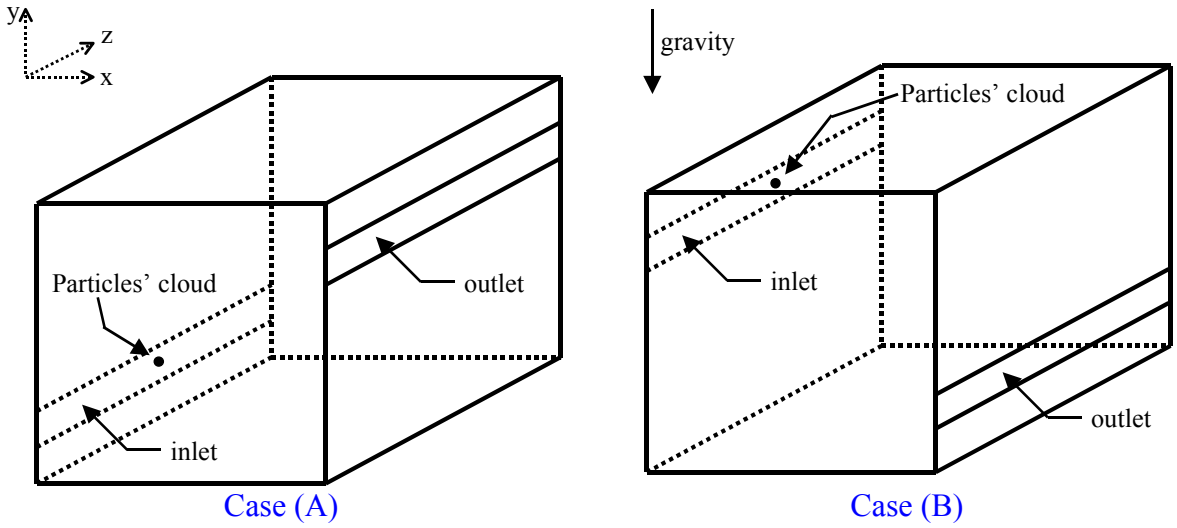

Fig. 4 Geometry of the ventilated rooms

Fig. 5 displays the mean velocity vectors in the vertical mid plane z=1.25m of the cavity, for Case (B). The main features of the cavity flow are the usual ones encountered in a ventilated cavity. The cavity flow consists of small recirculation regions in the corners of the cavity and a big one in the room core.

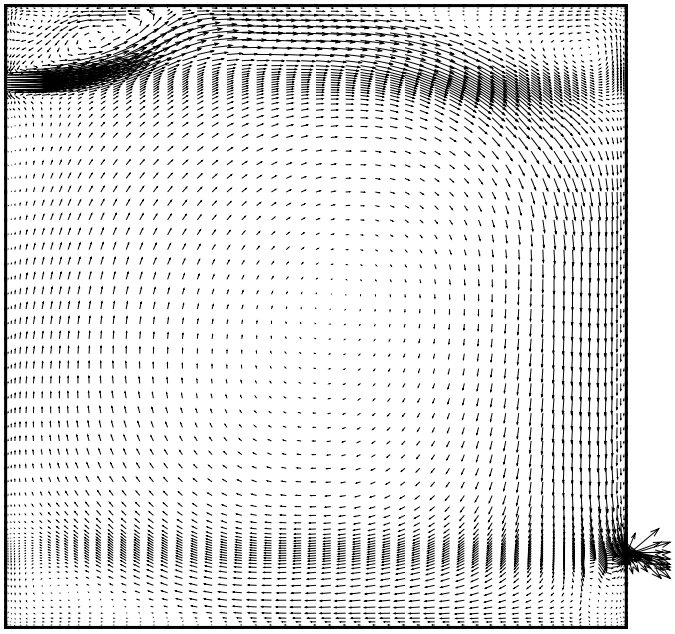

Fig. 5 Mean velocity field (Case (B), inlet : top, outlet : bottom)

Fig. 6 presents the temporal evolution of the particles' cloud in the room, for the 5µm particles and Case (A), inlet : bottom, outlet : top. Since these particles are light, they follow the air movement. About 10s since the particles' injection, a few particles are captured in the small recirculation regions in the bottom left and right corners. Fig. 6 (b) shows the particles going up along the right wall. One notices that some particles are exhausted. 30s since the particles' injection, particles spread to the big recirculation region. Fig. 7 gives the temporal evolution of the percentage of particles stuck on every surface, exhausted, and in the air flow. In this figure, it is observed that particles are eliminated mainly because they are exhausted. Only a very small percentage of particles stick to the surfaces of the cavity. The same remarks as for Fig. 7 can be done when examining the statistical results obtained for the 5µm particles and Case (B), inlet : top, outlet : bottom (see Fig. 8) : the particles follow the jet path and disappear from the room because they reach the outlet. For these light particles, the statistical results are almost the same, the locations of the inlet and outlet do not influence these results and thus indoor air quality.

Fig. 9 displays the temporal evolution of the 20 µm particles' cloud in the room, for Case (A), inlet : bottom, outlet : top. The air jet is strong enough to lift some particles along the right vertical wall, and a few ones will be exhausted. But for this case, the gravity force acts on the particles and very soon since the particles' injection, particles are eliminated because they deposit to the floor. Once the particles reach the outlet, a few ones are exhausted (see the percentage of particles exhausted and stuck on the floor, according to time, in Fig. 10). Fig. 11

shows the temporal evolution of the 20 μm particles' cloud in the room, for case (b) (inlet : top, outlet : bottom). As highlighted for previous cases, particles follow the jet path. A few particles are entrapped in the recirculation region in the upper left corner of the cavity. Particles go down along the right vertical wall, and some particles are caught by the outlet. In addition, due to the combined effects of the air jet going down the right wall and of the gravity force, many particles are driven to the outlet, and only a small percentage of particles deposit to the floor (see the temporal evolution of the percentage of particles exhausted and stuck on the floor in Fig. 12). A comparison between Fig. 10 and Fig. 12 shows that the ventilation scenario affects the percentage of particles in the air. For this case of particles' pollution (heavy particles emitted by ventilation), the percentage of particles in the air is smaller if the inlet is in the lower part of the left wall and the outlet is in the upper part of the right wall. But it should be kept in mind that for this case, many particles are deposited on the floor and are not removed from the room.

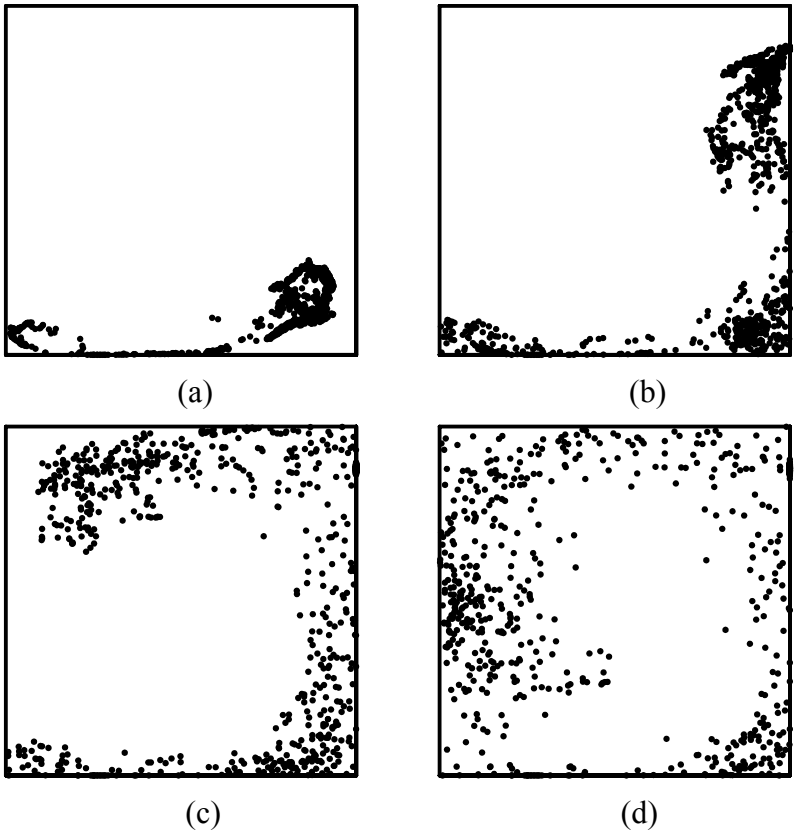

Fig. 6 Temporal evolution of the particles' cloud in the room
(a) 5s., (b) 10s., (c) 20s., (d) 30s.
(5 μm particles; Case (A), inlet : bottom, outlet : top)

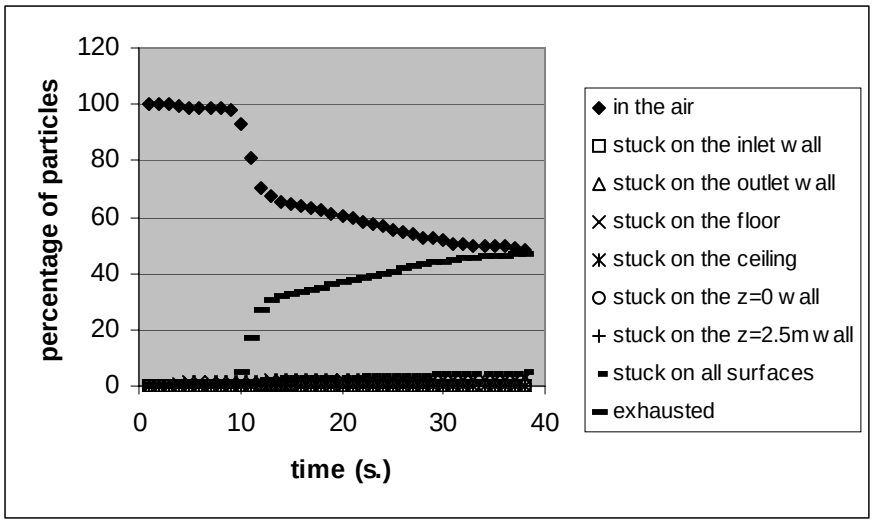

Fig. 7 Temporal evolution of the particle statistical results
(5 μm particles; Case (A), inlet : bottom, outlet : top)

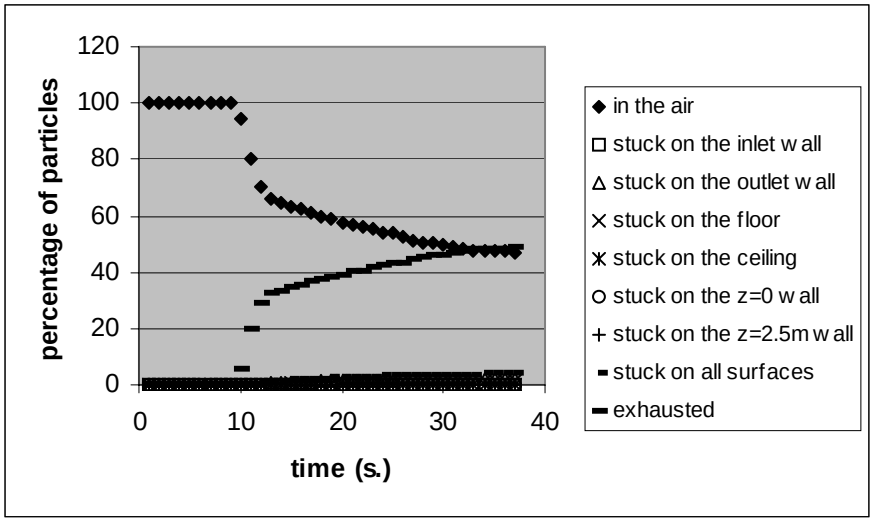

Fig. 8 Temporal evolution of the particle statistical results
(5 μm particles; Case (B), inlet : top, outlet : bottom)

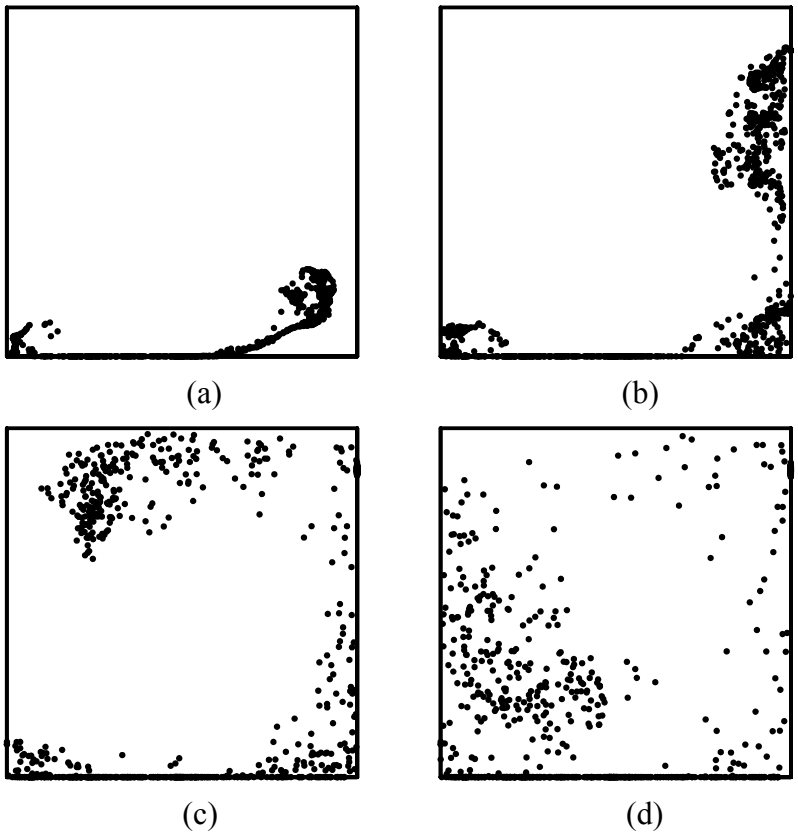

Fig. 9 Temporal evolution of the particles' cloud in the room
(a) 5s., (b) 10s., (c) 20s., (d) 30s.
(20 μm particles; Case (A), inlet : bottom, outlet : top)

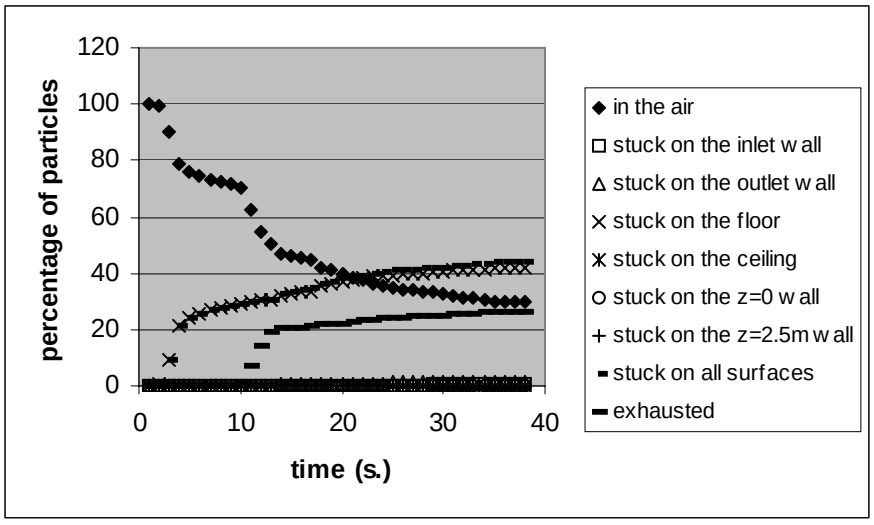

Fig. 10 Temporal evolution of the particle statistical results
(20 μm particles; Case (A), inlet : bottom, outlet : top)

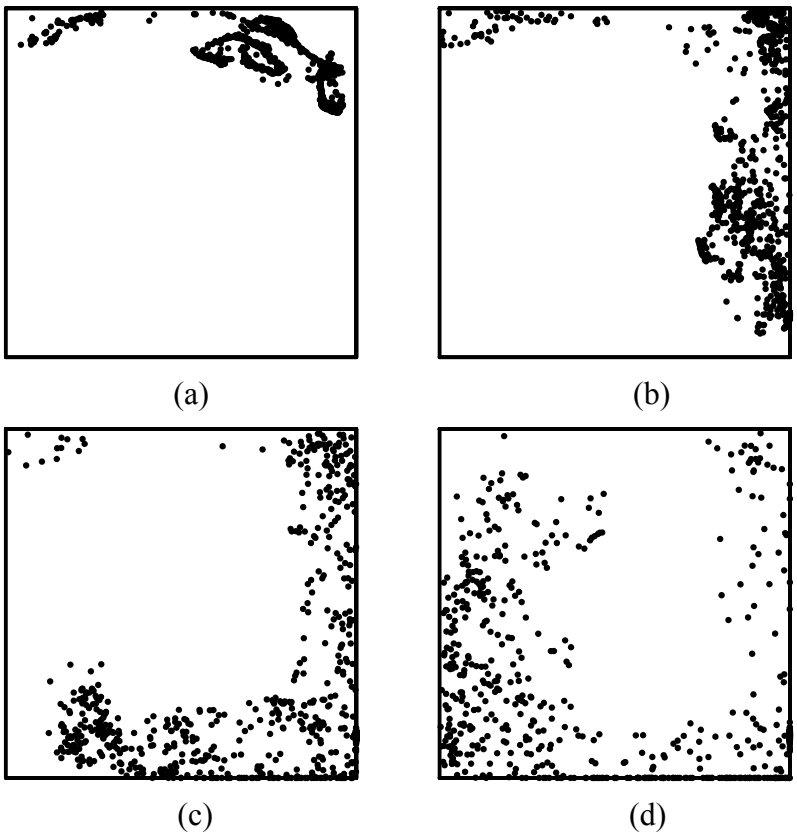

Fig. 11 Temporal evolution of the particles' cloud in the room
(a) 5s., (b) 10s., (c) 20s., (d) 30s.
(20 μm particles; Case (B), inlet : top, outlet : bottom)

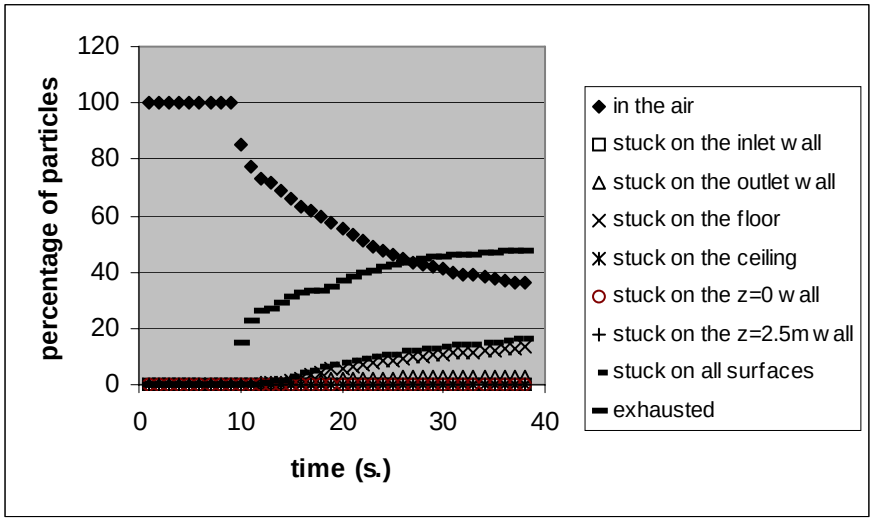

Fig. 12 Temporal evolution of the particle statistical results
(20 μm particles; Case (B), inlet : top, outlet : bottom)

5. Conclusions and future work

This paper describes how to use a large eddy simulation (LES) program with a Lagrangian particle model to simulate particle dispersion in a ventilated room.

The motion of three different types of solid particles in a decaying homogeneous isotropic turbulent airflow was first calculated. By comparing the computed results with the experimental data from the literature, the LES program is verified to be a successful tool to predict correctly the particle motion with regard to the second-order statistics, such as the mean-square displacement and turbulent intensity. The LES program was then applied successfully to investigate particle dispersion in a ventilated room. This model is thus a powerful tool to study particle dispersion in a room.

However, it was found that the computing costs are high, since the integration of the particles' equations of motion requires a very small time step. In order to increase the time step (and to save computing time), it will be interesting to test the exponential lagrangian tracking schemes proposed by Barton (Barton, 1996). Another alternative that enables to save computing time and to keep the benefits of large eddy simulation is to build a low dimensional dynamic model (obtained by projecting the Navier-Stokes equations onto a specific basis derived by proper orthogonal decomposition for instance) to compute the instantaneous fluid velocities at the particle's location (for further details, see Allery *et al.*, 2005).

Acknowledgments

This work is supported by Lincoln Laboratory, Massachusetts Institute of Technology (MIT). We wish to express our thanks to the Conférence des Grandes Ecoles, France, which funded Claudine Béghein's visit to MIT as a Visiting Scholar. Part of the computations was performed on the IBM SP supercomputer of the CINES (Centre Informatique de l'Enseignement Supérieur, France).

References

Abadie M., Limam K., Allard F. (2001) "Indoor particle pollution: effect of wall textures on particle deposition", Building and Environment 36, 821-827.

Allery, C., Béghein, C., and Hamdouni, A. (2005) "Applying proper orthogonal decomposition to the computation of particle dispersion in a two-dimensional ventilated cavity", Communications in Nonlinear Science and Numerical Simulation 10 (8), 907-920.

Armenio, V., Piomelli, U., and Fiorotto, V. (1999) "Effect of the subgrid scales on particle motion," Phys. Fluids, 11, 3030-3042.

ASHRAE Fundamentals Handbook, Ventilation and infiltration, American Society of Heating, Refrigerating and Air-Conditioning Engineers, Inc., Atlanta, GA, 1997.

Barton, I.E. (1996) "Exponential lagrangian tracking schemes applied to Stokes law", Journal of Fluids Engineering 118, 85-89.

Berlemont, A., Desjonqueres, P., and Gouesbet, G. (1990) "Particle Lagrangian simulation in turbulent flows," Int. J. Multiphase Flow 16, 19-34.

Crowe, C., Sommerfeld, M., and Tsuji, Y. (1998) *Multiphase flows with droplets and particles*, CRC Press, Boca Raton, Florida.
Deardorff, J.W. (1970) "A numerical study of three-dimensional turbulent channel flow at large Reynolds numbers," J. Fluid Mech. 41, 453-480.
Emmerich, S.J. and McGrattan, K.B. (1998) "Application of a large eddy simulation model to study room airflow," ASHRAE Transactions 104, 1128-1140.
Harlow F.H. and Welch, J.E. (1965) "Numerical calculation of time-dependent viscous incompressible flow," Phys. Fluids 8 (12), 2182-2189.
Hinds, W.C. (1982) *Aerosol technology : properties, behaviour, and measurement of airborne particles*, John Wiley and Sons, Inc.
Hjelmfelt, A.T. and Mockros, L.F. (1966) "Motion of discrete particles in a turbulent fluid," App. Sci. Res., 16, 149.
Holub, R.F., Raes, F., Van Dingenen, R., and Vanmarcke, H. (1988) "Deposition of aerosols and unattached radon daughters in different chambers: theory and experiment," Radiation Protection Dosimetry, 24, 217-220.
Jiang, Y. and Chen, Q. (2001) "Study of natural ventilation in buildings by large eddy simulation," J. Wind Eng. Ind. Aerodyn. 89 (13), 1155-1178.
Jiang, Y. and Chen, Q. (2002) ""Study of cross natural ventilation in a building site by large eddy simulation," Building and Environment, 37, 379-386.
Jiang, Y. and Chen, Q. (2003) "Buoyancy driven single sided natural ventilation in buildings with large openings", International J. of Heat and Mass Transfer, 46, 973-988.
Klose, G., Rembold, B., Koch, R., Wittig, S. (2001) "Comparison of state of the art droplet turbulence interaction models for jet engine combustor conditions," International Journal of Heat and Fluid Flow, 22, 343-349.
Lakehal, D. and Rodi, W. (1997) "Calculation of the flow past a surface-mounted cube with two-layer turbulence models," J. Wind Eng. Ind. Aerodyn. 67/68, 65-78.
Lu, Q.Q., Fontaine, J.R., Aubertin, G. (1993) "A lagrangian model for solid particles in turbulent flows," Int. J. Multiphase Flow, 19 (2), 347-367.
Mc Laughlin, J.B. (1989) "Aerosol deposition in a numerically simulated channel flow", Physics of Fluids, A 1 (7), 1211-1224.
Mittal, P. and Moin, P. (1997), "Suitability of upwind-based finite-difference schemes for large eddy simulation of turbulent flows," AIAA J. 35 (8), 1415-1417.
Okuyanna, K., Kousaka, Y., Yamamoto, S., and Hosokaya, T. (1986) "Particle loss of aerosols in a stirred tank," J. Chemical Eng. Japan, 10(2), 142-147.
Pozorski, J., Minier, J.P. (1998) "On the lagrangian turbulent dispersion models based on the Langevin equation," Int. J. Multiphase Flow, 24, 913-945.
Riley, J.J., and Patterson, G.S. (1974) "Diffusion experiments with numerically integrated isotropic turbulence," Phys. Fluids 17(2), 292-297.
Rodi, W., Ferziger, J.H., Breuer M., and Pourquié, M. (1997) "Status of large eddy simulation: results of a workshop," J. Fluids Eng., 119, 248-262.
Saffman, P.G. (1965) "The lift of a sphere in a slow shear flow", Journal of Fluid Mechanics, 22 (2), 385-400.
Shah, K.B. (1998) *Large eddy simulations of flow past a cubic obstacle*. Ph.D. dissertation, Department of Mechanical Engineering, Stanford University, USA.
Smagorinsky, J., (1963) "General circulation experiments with the primitive equations. I. The basic experiment," Monthly Weather Review 91, 99-164.

Snyder, W.H. and Lumley, J.L. (1971) “Some measurements of particle velocity autocorrelation functions in a turbulent flow,” J. Fluid Mech. 48 (1), 41-71.
Stone, H.L. (1968) “Iterative solution of implicit approximations of multidimensional partial differential equations,” SIAM J. Numerical Analysis 5 (3), 530-558.
William, H. (1992) *Numerical recipes in FORTRAN : the art of scientific computing*, Cambridge University Press, Cambridge [England] ; New York, NY, USA.
Zhang, W. and Chen, Q., (2000) “Large eddy simulation of indoor airflow with a filtered dynamic subgrid scale model,” International J. of Heat and Mass Transfer 43 (17), 3219-3231.